

## On the influence of fires on cloud and precipitation formation\*

O.A. Dubrovskaja, A.A. Lezhenin, V.M. Mal'bakhov, V.A. Shlychkov

**Abstract.** During forest fires the heat, moisture, and aerosols are carried out to the troposphere due to the intensive convective activity above zones of burning. The influence of these substances on processes of cloud and precipitation formation is studied with the help of numerical eddy-resolving model of the atmospheric boundary layer. It is shown that heat and moisture coming from the fire zone intensify the cloud formation processes, while aerosol fills up the atmosphere by water vapor condensation nucleus what results in formation of small suspended droplets below zero isotherm level. If the cloud top is overcooled (just such clouds give intensive precipitation), a plenty of aerosol particles, more than 1 micron in size getting here, causes a crystallization of overcooled drops and precipitation subsiding or stopping.

Analysis of satellite data shows a considerable decrease in precipitation sum over the territory, where forest fires occur [1]. There are two mechanisms of such an influence:

- atmospheric circulation change due to the heat release during natural fires;
- the influence of a large amount of smoke aerosol on the processes of cloud and precipitation formation on regional scale.

Space images of the Yakut fires of 2002 demonstrate, in some cases, formation of convective clouds above a fire. The theory speaks [2] that above a fire zone there can be a convective column which reaches the height of more than one kilometer. Under favorable conditions, the water vapor, steamed during burning, reaches a condensation level and facilitates formation of cumulus clouds which can precipitate. The direct thermal and dynamic influence of forest fires on the processes of cloud and precipitation formation [2] is limited by a local area above the fire. Thus, fires intensify these processes. Satellite images of forest fires show that in some cases there is a convective cloud above a burning zone.

Forest fires significantly pollute the air with gaseous, liquid and solid products of burning. The length of smoke plume from a forest fire can be more than 100 km, and at mass fires, the area of the smoke cover exceeds  $10^6$  km<sup>2</sup>, as in the case of the Yakut fires of 2002. According to field data [1] and results of [2], the smoke from intensive fires can reach the height of a few

---

\*Supported by the Russian Foundation for Basic Research under Grant 03-05-65279.

kilometers and participate in the processes of precipitation formation. The greatest influence on the processes of precipitation formation is rendered by aerosol solid particles. Usually, the solid aerosol is divided into three fractions: fine, intermediate, and coarse, each influencing in a different way on the processes of cloud and precipitation formation [3]. The contribution of these aerosol fractions to different types of smoke is presented in the table.

Percentage of three fractions of solid aerosol for different smoke types

Particle fraction	Particle radius, micron	Contribution of fractions to smoke volume, %		
		Light smoke	Dense smoke	"Old" smoke
Fine	0.03–0.06	95–98	1–2	2–3
Middle	0.3–0.5	2–5	3–5	18–20
Coarse	1.0–1.5	—	90–95	75–80

The water vapor condensates on impurity particles of a fine fraction, while intermediate and coarse aerosol particles serve as nucleus of water droplets coagulation. An increase in the rate of vapor condensation and water drops coagulation of result in intensification of processes of precipitation formation in the lower part of the cloud relatively to its warm part. The upper boundary of rain clouds in the middle and high latitudes has a height from 5 up to 10 km. The upper part of such clouds consists of water vapor, water drops, ice crystals, snow, and ice sleet [4]. According to experimental data [4], the formation of ice crystals requires the presence of sufficiently coarse aerosol particles in the atmosphere. Actually, the plane surveys evidences that ice crystals are observed when the cloud reaches the height, where the temperature is lower than  $-12^{\circ}\text{C}$ . This very value is the highest temperature at which introduction of the insignificant amount of particles of ground, mineral dust, and soot is sufficient for visual appearance of ice crystals in a laboratory cloud [4].

The table shows that with an increase of the smoke cover density, smoke becomes more and more coarse [4]. The concentration of a coarse aerosol of 100 particles /  $1\text{ m}^3$  is sufficient to provide the occurrence of a necessary amount of ice-generating crystals. This amount of particles is released to the atmosphere at the height of isotherm  $-12^{\circ}\text{C}$  during large fires, and makes several hundreds of one percent of the burned down biomass.

Thus, the influence of smoke aerosol on the processes of cloud and precipitation formation is determined by:

- the presence of a plenty of coarse aerosol particles in the forest fire smoke;
- entering aerosol coarse fractions with convective streams to the middle layers of the atmosphere, where clouds develop.

This provides a formation of ice-generating crystals in the overcooled part of the cloud and the influence of ice crystals on processes of cloud and precipitation formation.

The objective of the present work is a theoretical study of the influence of coarse aerosol particles on the processes of precipitation formation. It is assumed that these aerosol particles of the assigned concentration get to the calculated area from a forest fire zone.

To obtain the initial system of equations, a spatial filter of the box type [5] is applied to the Navier–Stokes equations for an incompressible fluid and unperturbed stably stratified “background” with fields of temperature, pressure and density introduced within the LES-approach [6]:

$$\begin{aligned}
 \frac{\partial u}{\partial t} + u \frac{\partial u}{\partial x} + v \frac{\partial u}{\partial y} + \frac{1}{\bar{\rho}} w \frac{\partial \bar{\rho} u}{\partial z} &= -c_p \bar{\Pi} \frac{\partial \pi}{\partial x} + lv - \frac{1}{\bar{\rho}} \left( \frac{\partial \tau_{xx}}{\partial x} + \frac{\partial \tau_{xy}}{\partial y} + \frac{\partial \tau_{xz}}{\partial z} \right), \\
 \frac{\partial v}{\partial t} + u \frac{\partial v}{\partial x} + v \frac{\partial v}{\partial y} + \frac{1}{\bar{\rho}} w \frac{\partial \bar{\rho} v}{\partial z} &= -c_p \bar{\Pi} \frac{\partial \pi}{\partial y} - lu - \frac{1}{\bar{\rho}} \left( \frac{\partial \tau_{yx}}{\partial x} + \frac{\partial \tau_{yy}}{\partial y} + \frac{\partial \tau_{yz}}{\partial z} \right), \\
 \frac{\partial w}{\partial t} + u \frac{\partial w}{\partial x} + v \frac{\partial w}{\partial y} + \frac{1}{\bar{\rho}} w \frac{\partial \bar{\rho} w}{\partial z} &= -c_p \bar{\Pi} \frac{\partial \pi}{\partial z} + \lambda \vartheta - \frac{1}{\bar{\rho}} \left( \frac{\partial \tau_{zx}}{\partial x} + \frac{\partial \tau_{zy}}{\partial y} + \frac{\partial \tau_{zz}}{\partial z} \right), \\
 \frac{\partial \vartheta}{\partial t} + u \frac{\partial \vartheta}{\partial x} + v \frac{\partial \vartheta}{\partial y} + \frac{1}{\bar{\rho}} w \frac{\partial \bar{\rho} \vartheta}{\partial z} + Sw &= -\frac{1}{\bar{\rho}} \left( \frac{\partial \sigma_x}{\partial x} + \frac{\partial \sigma_y}{\partial y} + \frac{\partial \sigma_z}{\partial z} \right) + \Phi_T, \\
 \frac{\partial \bar{\rho} u}{\partial x} + \frac{\partial \bar{\rho} v}{\partial y} + \frac{\partial \bar{\rho} w}{\partial z} &= 0,
 \end{aligned} \tag{1}$$

where  $u, v, w$  are velocity vector components along the axes  $x, y, z$ ;  $\vartheta$  is a perturbation of potential temperature,  $l$  is the Coriolis parameter,  $\lambda$  is the buoyancy parameter,  $c_p$  is a specific thermal air capacity at constant pressure,  $S = \partial \Theta / \partial z$  is temperature stratification,  $\Phi_T$  is phase inflow of heat,  $\tau_{ij}$  are components of the turbulent stress tensor,  $\Theta, T, P, \Pi$  are potential temperature, absolute temperature, pressure, the Exner function (pressure analogue), respectively, variables with a bar are the background fields satisfying the equations of condition and statics

$$\bar{P} = R_a \bar{\rho} \bar{T}, \quad \frac{d\bar{P}}{dz} = -\bar{\rho} g, \quad \bar{\Pi} = \frac{\bar{\Theta}}{\bar{T}}, \tag{2}$$

where  $\bar{\rho}(z)$  is a static fall of density with a height,  $g$  is gravity acceleration,  $R_a$  is a gas constant. This system of equations is a basis for building a mesoscale model of the atmospheric boundary layer (LBL).

The equations system for humidity and precipitation transport is considered together with the equations of the ABL hydrothermodynamics (1) and contains the equations for water vapor  $q$ , the weighted drop  $q_c$  and the crystal moisture  $q_i$ , the liquid precipitations  $q_r$  and snow  $q_s$ .

$$\begin{aligned}
\frac{dq}{dt} &= D_{xy}q + \frac{1}{\bar{\rho}} \frac{\partial}{\partial z} \bar{\rho} K_H \frac{\partial q}{\partial z} - \Phi_1 - \Phi_2 - \Phi_3 - \Phi_4 - \Phi_5 - \Phi_6, \\
\frac{dq_c}{dt} &= D_{xy}q_c + \frac{1}{\bar{\rho}} \frac{\partial}{\partial z} \bar{\rho} K_H \frac{\partial q_c}{\partial z} + \Phi_1 + \Phi_7 - \Phi_8 - \Phi_9 - \Phi_{10}, \\
\frac{dq_i}{dt} &= D_{xy}q_i + \frac{1}{\bar{\rho}} \frac{\partial}{\partial z} \bar{\rho} K_H \frac{\partial q_i}{\partial z} + \Phi_1 + \Phi_5 - \Phi_7 + \Phi_8 - \Phi_{11} - \Phi_{12}, \\
\frac{dq_r}{dt} - \frac{1}{\bar{\rho}} \frac{\partial \bar{\rho} W_r q_r}{\partial z} &= D_{xy}q_r + \frac{1}{\bar{\rho}} \frac{\partial}{\partial z} \bar{\rho} K_H \frac{\partial q_r}{\partial z} + \Phi_2 + \Phi_8 + \Phi_9 + \Phi_{10} - \Phi_{13}, \\
\frac{dq_s}{dt} - \frac{1}{\bar{\rho}} \frac{\partial \bar{\rho} W_s q_s}{\partial z} &= D_{xy}q_s + \frac{1}{\bar{\rho}} \frac{\partial}{\partial z} \bar{\rho} K_H \frac{\partial q_s}{\partial z} + \Phi_3 + \Phi_4 + \Phi_{10} + \Phi_{11} + \Phi_{12} + \Phi_{13},
\end{aligned} \tag{3}$$

where  $\Phi_i$  ( $i = 1, \dots, 13$ ) are velocities of phase transformations,  $W_r$ ,  $W_s$  are velocities of gravitational rain and snow deposition,  $\frac{d}{dt}$  is the individual derivative operator,  $K_H$  is a vertical turbulent exchange coefficient for  $q$ ,  $q_c$ ,  $q_i$ ,  $q_r$ ,  $q_s$ ;

$$D_{xy} = \frac{1}{\bar{\rho}} \left( \frac{\partial}{\partial x} \bar{\rho} K_H \frac{\partial}{\partial x} + \frac{\partial}{\partial y} \bar{\rho} K_H \frac{\partial}{\partial y} \right)$$

is the turbulent exchange operator along  $x$ ,  $y$ . For the quantitative description of  $\Phi_i$ , one-parametrical laws of distribution of liquid and solid precipitation are assigned according to the dependencies [7]

$$N_r = N_{0r} \exp(-\lambda_r D_r), \quad N_s = N_{0s} \exp(-\lambda_s D_s),$$

where  $N_{0r}$ ,  $N_{0s}$  is a maximum concentration of liquid and crystal particles of precipitation in the Marshall–Palmer distribution,  $D_r$ ,  $D_s$  are diameters of particles. Omitting here bulky expressions for  $\Phi_i$ , we specify their semantic content [7]:

- $\Phi_1$  is the water vapor condensation rate ( $\Phi_1 > 0$ ) into a cloudy moisture or a cloudy water evaporation ( $\Phi_1 < 0$ );
- $\Phi_2$  is the condensation (evaporation) water vapor rate on rain drops;
- $\Phi_3$  is deposition of water vapor on particles of snow, or sublimation of snow;
- $\Phi_4$  is the snow evaporation rate at thawing ( $T \geq 0^\circ\text{C}$ );
- $\Phi_5$  is the vapor deposition rate on cloudy crystals ( $T \leq T_f$ ), or evaporation of ice;
- $\Phi_6$  is activation of ice crystals ( $T < 0^\circ\text{C}$ );
- $\Phi_7$  is describes the thawing of cloud crystals ( $T \geq 0^\circ\text{C}$ );
- $\Phi_8$  is describes the process of autoconversion (coalescence) of cloud drops ( $T \geq 0^\circ\text{C}$ );

- $\Phi_9$  is velocity of capture of cloud drops by the rain (accretion);
- $\Phi_{10}$  is velocity of capture of liquid cloud drops by snow particles ( $T_f \leq T \leq 0^\circ\text{C}$ );
- $\Phi_{11}$  is capture of ice crystals by snow ( $T \leq 0^\circ\text{C}$ );
- $\Phi_{12}$  is aggregation of cloud crystals into the snow ( $T \leq 0^\circ\text{C}$ );
- $\Phi_{13}$  is the snow thawing rate with transition into the rain ( $T \geq 0^\circ\text{C}$ ) or transformation of rain drops into snow crystals  $T \leq 0^\circ\text{C}$ .

Here  $T$  is the temperature of the air-droplet mix in Centigrade degrees,  $T_f \approx -10^\circ\text{C}$  is the threshold temperature below which the processes of condensation on the overcooled liquid-droplet moisture are replaced by the processes of dry distillation of vapor into ice. At  $T > 0$ , cloud drops and liquid precipitation are supposed to occur at  $T_f < T < 0$ , clouds form overcooled drops and ice crystals, and at  $T < T_f$ , both clouds and precipitation have a crystal structure. The block of phase transitions of the moisture includes: water vapor, liquid and crystal phases of clouds, and heavy fractions of rain and snow, as seen in Figure 1.

Let us assign the edge conditions for equations (1)–(3) with allowance for moisture exchange parametrization in the layer of constant streams:

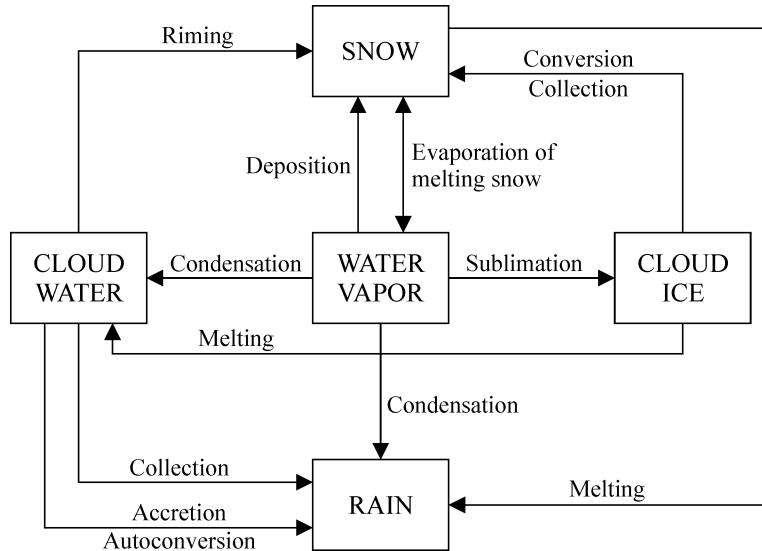


**Figure 1.** Interconversions in the system “vapor, water, ice”

$$\begin{aligned}
K_H \frac{\partial q}{\partial z} &= C_\Theta |\vec{U}| (q - q_0), \quad \tau_{xz} = C_{u\rho} |\vec{U}| u, \quad \tau_{yz} = C_{u\rho} |\vec{U}| v, \\
w = 0, \quad \frac{\partial q_c}{\partial z} &= \frac{\partial q_i}{\partial z} = \frac{\partial q_r}{\partial z} = \frac{\partial q_s}{\partial z} = 0, \quad \vartheta = 0 \quad \text{at } z = h; \\
w = 0, \quad q &= q_H, \quad q_c = q_i = q_r = q_s = 0, \quad \frac{\partial \theta}{\partial z} = \gamma \quad \text{at } z = H,
\end{aligned} \tag{4}$$

where  $q_0$  is specific humidity near to the underlying surface,  $q_H$  is the assigned distribution of humidity in the free atmosphere,  $\theta_0(t)$  assigns a daily temperature trend at  $z = h$ ;  $\gamma$  assigns a stable stratification at large heights. On the lateral boundaries of the calculated area we accept the conditions when the normal derivatives of required functions are equal to zero. The way of assigning the vertical heat and moisture distribution is given in [8]. The grid  $1 \times 32$  detalization in the horizontal plane and 100 levels in the vertical plane in the area of  $80 \times 10 \times 10 \text{ km}^3$  allow the obvious resolution of coherent structures in a stochastic convective-cloud ensemble.

Model (1)–(4) was used for a comparative analysis of precipitation sum and distribution in the presence of various impurity concentration in the atmosphere. The occurrence of cloudiness was simulated by assignment of overheating  $T_h$  at  $z = h$  in a local part of the space  $R$  with the size  $10 \times 10 \text{ km}$  along  $x$  and  $y$ , respectively:

$$\begin{aligned}
x, y \in R \quad \text{at } z = h, \quad \vartheta &= T_k, \\
x, y \notin R \quad \text{at } z = h, \quad \vartheta &= 0.
\end{aligned}$$

A series of experiments was performed with the assignment of the following overheating values:  $T_h = 5^\circ\text{C}$ ,  $T_h = 7^\circ\text{C}$ ,  $T_h = 9^\circ\text{C}$ . Calculations were carried out for 1.5 hours. The results obtained have shown that in a few minutes, overheating causes the formation of a convective ensemble that initially consists only of thermics. Then, when most “powerful” thermics reaches the condensation level, convective clouds start to form. The vertical sizes of clouds increase, and in 20–30 minutes precipitation starts to drop out from them. The precipitation intensity essentially depends on a height of the upper edge of clouds  $H_0$ , which is about 4 km at  $T_h = 5^\circ\text{C}$ , about 5 km at  $T_h = 7^\circ\text{C}$ , and about 6 km at  $T_h = 9^\circ\text{C}$ . The precipitations sum in millimeters at different moments of time for these overheating values are given in Figure 2. The figure shows that with the absence of impurity in clouds in the 1st case, 15 mm precipitation has dropped out, in the 2nd case – 20 mm, in the 3rd case – 25 mm. The introduction of coarse particles of impurity in all the three cases resulted in reduction of precipitation. In the first case, concentration of 100 particles /  $1 \text{ m}^3$  turned to be sufficient for the reduction of precipitation by 10%. In the second and the third cases, the same concentration of particles has reduced the precipitation sum by 20%.

On the basis of the results of numerical experiments, it is possible to draw the following conclusion: if a cloud has the overcooled top (these very clouds

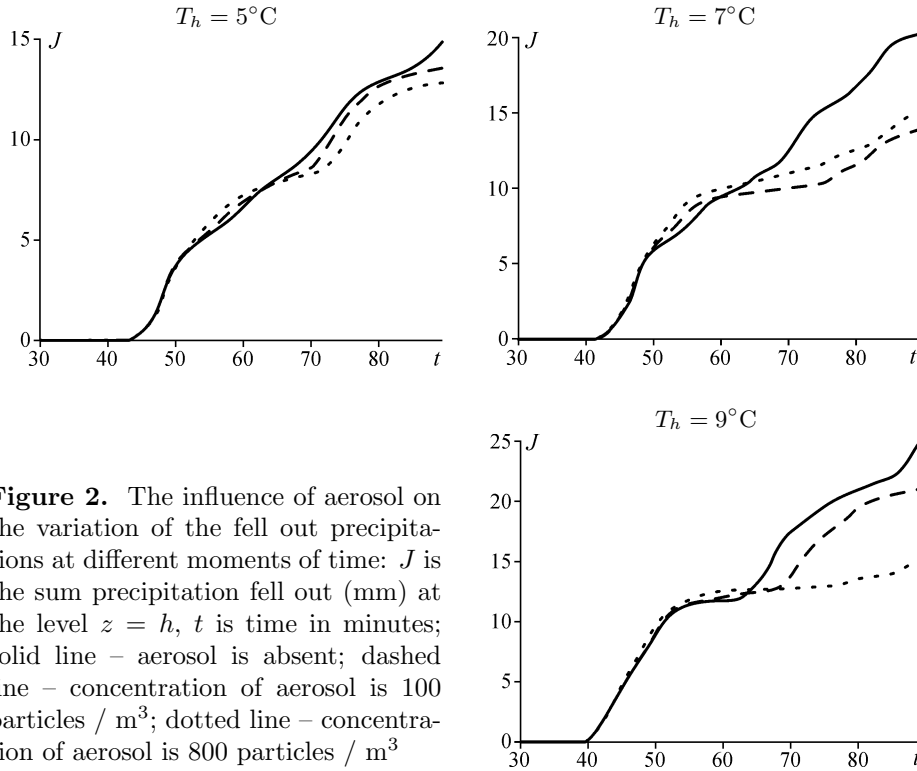


**Figure 2.** The influence of aerosol on the variation of the fell out precipitations at different moments of time:  $J$  is the sum precipitation fell out (mm) at the level  $z = h$ ,  $t$  is time in minutes; solid line – aerosol is absent; dashed line – concentration of aerosol is 100 particles /  $\text{m}^3$ ; dotted line – concentration of aerosol is 800 particles /  $\text{m}^3$

give an intensive precipitation), the aerosol particles with sizes exceeding 1 micron result in precipitation reduction. The presence of aerosol results in the fast crystallization of water droplets in the upper part of a cloud. Such clouds give weaker precipitation than those whose tops consist of ice crystals, snow, and rain drops.

## References

- [1] Sukhinin A.I. Yakut fires of 2002 as prototypes of global ecological accidents // Materials of 5th International Conference “Natural fires: occurrence, distribution, suppression and ecological consequences”. — Tomsk: Tomsk University, 2003. — P. 181–182.
- [2] Mal’bakhov V.M., Shlychkov V.A. Calculation of rise height of smoke aerosol involved in cloud systems in forest fire zone // Optics of the Atmosphere and the Ocean. — 2004. — No. 17. — P. 453–456.
- [3] Kozlov V.S., Panchenko M.V. Research of optical properties and disperse structure of wood smoke aerosols // Physics of Burning and Explosion. — 1996. — Vol. 32, No. 5. — P. 122–133.

- [4] Mason B.J. *Physics of Clouds*. — Leningrad: Hydrometeorological Publishing House, 1961.
- [5] *Atmospheric Turbulence and Modeling of Impurity. Distribution*. — Leningrad: Hydrometeorological Publishing House, 1985.
- [6] Moeng C.-H. A large-eddy-simulation model for the study of planetary boundary layer turbulence // *J. Atmos. Sci.* — 1984. — Vol. 41, No. 13. — P. 2052–2062 (LIT the Siberian Branch of the Russian Academy of Science).
- [7] Rutledge S.A., Hobbs P.V. The mesoscale and microscale structure and organization of clouds and precipitation in midlatitude cyclones. VIII: A model for the “seeder-feeder” process in warm-frontal rainbands // *J. Atmos. Sci.* — 1983. — Vol. 40, No. 5. — P. 1185–1206.
- [8] Shlychkov V.A., Pushistov P.Yu., Mal'bakhov V.M. The influence of atmospheric convection on vertical transport of arid aerosols // *Optics of the Atmosphere and the Ocean*. — 2001. — Vol. 14, No. 6–7. — P. 578–582.